Mathematical Biosciences and Engineering

MBE, 19(9): 9295–9320.
DOI: 10.3934/mbe.2022432
Received: 08 March 2022
Revised: 15 June 2022
Accepted: 16 June 2022
Published: 24 June 2022

http://www.aimspress.com/journal/MBE

Research article

FMR1 is identified as an immune-related novel prognostic biomarker for renal clear cell carcinoma: A bioinformatics analysis of TAZ/YAP

Sufang Wu[1,2], Hua He[1,2], Jingjing Huang[1,2], Shiyao Jiang[1,2], Xiyun Deng[1,2], Jun Huang[3], Yuanbing Chen[3,*] and Yiqun Jiang[1,2,*]

[1] The Key Laboratory of Model Animal and Stem Cell Biology in Hunan Province, Hunan Normal University, Changsha 410013, Hunan, China
[2] School of Medicine, Hunan Normal University, Changsha 410013, Hunan, China
[3] Department of Neurosurgery, Xiangya Hospital, Central South University, Changsha 410008, Hunan, China

* **Correspondence:** Email: jiangyiqun@hunnu.edu.cn, chenyuanbing@csu.edu.cn.

Abstract: WW domain-containing transcription regulator 1 (TAZ, or WWTR1) and Yes-associated protein 1 (YAP) are both important effectors of the Hippo pathway and exhibit different functions. However, few studies have explored their co-regulatory mechanisms in kidney renal clear cell carcinoma (KIRC). Here, we used bioinformatics approaches to evaluate the co-regulatory roles of TAZ/YAP and screen novel biomarkers in KIRC. GSE121689 and GSE146354 were downloaded from the GEO. The limma was applied to identify the differential expression genes (DEGs) and the Venn diagram was utilized to screen co-expressed DEGs. Co-expressed DEGs obtained the corresponding pathways through GO and KEGG analysis. The protein-protein interaction (PPI) network was constructed using STRING. The hub genes were selected applying MCODE and CytoHubba. GSEA was further applied to identify the hub gene-related signaling pathways. The expression, survival, receiver operating character (ROC), and immune infiltration of the hub genes were analyzed by HPA, UALCAN, GEPIA, pROC, and TIMER. A total of 51 DEGs were co-expressed in the two datasets. The KEGG results showed that the enriched pathways were concentrated in the TGF-β signaling pathway and endocytosis. In the PPI network, the hub genes (STAU2, AGO2, FMR1) were identified by the MCODE and CytoHubba. The GSEA results revealed that the hub genes were correlated with the signaling pathways of metabolism and immunomodulation. We found that STAU2 and FMR1 were weakly expressed in tumors and were negatively associated with the tumor stages. The overall survival (OS) and disease-free survival (DFS) rate of the high-expressed group of FMR1 was greater than that

of the low-expressed group. The ROC result exhibited that FMR1 had certainly a predictive ability. The TIMER results indicated that FMR1 was positively correlated to immune cell infiltration. The abovementioned results indicated that TAZ/YAP was involved in the TGF-β signaling pathway and endocytosis. FMR1 possibly served as an immune-related novel prognostic gene in KIRC.

Keywords: TAZ; YAP; FMR1; immune infiltrates; KIRC; bioinformatic analysis

Abbreviations: AUC: Area under the curve; ANOVA: One-way analysis of variance; AGO2: Argonaute RISC catalytic component 2; BP: Biological processes; CC: Cellular components; CI: Confidence interval; DEGs: Differential expression genes; DFS: Disease-free survival; DFELMDA: Deep forest ensemble learning based on autoencoder; FC: Fold change; FDR: False discovery rate; FMR1: Fragile X mental retardation 1; GEO: Gene expression omnibus; GTEx: Genotype-tissue expression; GEPIA: Gene expression profiling interactive analysis; GSEA: Gene set enrichment analysis; GO: Gene ontology; HPA: Human protein atlas; KIRC: Kidney renal clear cell carcinoma; KIRP: Kidney renal papillary cell carcinoma; KICH: Kidney chromophobe; KEGG: Kyoto encyclopedia of genes and genomes; Limma: Linear models for microarray data; LMFNRLMI: Logistic matrix factorization with neighborhood regularized; MCODE: Molecular complex detection; MSigDB: Molecular signatures database; MF: Molecular functions; NES: Normalized enrichment score; NDALMA: LncRNA–miRNA association prediction; OS: Overall survival; PPI: Protein-protein interaction; PDL1: Programmed cell death ligand 1; RCC: Renal cell carcinoma; ROS: Reactive oxygen species; ROC: Receiver operating character; STRING: Search tool for the retrieval of interacting genes; STAU2: Staufen double-stranded RNA binding protein 2; TCGA: The cancer genome atlas; TIMER: Tumor immune estimation resource; TAZ: WW domain-containing transcription regulator 1; VEGFA: Vascular endothelial growth factors A; YAP: Yes-associated protein 1

1. Introduction

Renal cell carcinoma (RCC) is the most prevalent and malignant solid tumor in the urinary system [1]. According to the statistics data of the 2020 global cancer report, the cases of birth and death are 431,288 and 179,368, respectively [2]; while the China statistic data show that there are approximately 73,587 birth cases and 43,196 death cases [3]. Generally, there are mainly three types of histologic features: kidney renal clear cell carcinoma (KIRC, 70%), kidney renal papillary cell carcinoma (KIRP, 10–15%), and kidney chromophobe (KICH, 5%) [4]. Currently, the first treatment choice is surgery in most KIRC patients; however, there is still a 30–40% recurrence rate in patients after surgery [5], with a 5-year overall survival (OS) rate of only approximately 12% [3]. Recently, emerging scholars have found that the changes in the tumor immune microenvironment were closely associated with the process of tumor [6,7]. Some researchers suggested that KIRC was an immune-infiltrated tumor [8]. The expression of immune-related genes was correlated with patients' prognosis [9,10]. The immune infiltration mediated approximately 1% of the spontaneous regression of patients [11]. Even though KIRC is one of the most sensitive tumors for immunotherapy, we are still unsatisfied with the clinical outcomes of patients [12]. Therefore, it is important to understand the regulatory mechanisms of the KIRC tumor immune microenvironment and identify immune-related prognostic biomarkers.

The Hippo pathway is a classic tumor suppressor signaling pathway to maintain the homeostasis of cells and organizations via regulating cell proliferation and differentiation, programmed cell death, immunity, metastasis, and chemotherapy suppression [13–15]. WW domain-containing transcription regulator 1 (TAZ, or WWTR1)/Yes-associated protein 1 (YAP) (homologous paralogues, partially common structures, and overlapping regulatory functions) are a type of transcriptional activators and both are essential Hippo pathway effectors [16]. When the Hippo pathway is activated, they are phosphorylated and degraded in the cytoplasm to inhibit the interaction with the TEA domain (TEAD) [17,18] or other transcription factors (paired box gene 3 (PAX3) [19,20], T-box transcription factor 5 (TBX5) [21,22], AP-1 [23] and SMADs [24]) in the nucleus, thereby influencing the homeostasis process of cells and organs through regulating the expression of common target genes. Recently, emerging evidence indicated that TAZ and YAP were the most common oncogenes. For example, a report stated that TAZ/YAP was inclined to interact with conserved enhancers and exhibited high chromatin profile activity in various cancers, which possibly was the fundamental reason to perturb the gene expression of cells [25]. Another report indicated that the TAZ/YAP mutation was tightly associated with six tumor development processes and immune cell infiltration [26]. However, it is intriguing that TAZ/YAP also possesses anti-cancer capacity. For example, TAZ/YAP contribute to ferroptosis and autophagy by regulating epithelial membrane protein 1 (EMP1)/angiopoietin-like 4 (ANGPTL4)-nicotinamide adenine dinucleotide phosphate (NADPH) oxidase 2 (NOX2) axis [27,28] and the expression of S-phase kinase-associated protein 2 (SKP2) [29] and LC3 [30], respectively. Presently, some studies, the combined analysis of TAZ/YAP, had revealed their common regulatory mechanisms. In cholangiocarcinoma, their low expressions inhibit the genes' expression of the cell cycle, DNA replication, and the Hippo pathway [31]. In RCC with neurofibromatosis type 2 (NF2) mutations, their depletions weaken the glycolysis and increase mitochondrial respiration and reactive oxygen species (ROS) to induce oxidative stress cell death [32]. In conclusion, it is complicated that TAZ/YAP was involved in the regulatory mechanisms. There are growing reports trying to understand their mechanisms and signaling pathways. However, due to some objective factors (cells' tolerance and sensitivity), it is not enough that we conduct the combined research of TAZ/YAP, so that we are incompletely clear about their specific regulatory mechanisms, especially in KIRC.

Bioinformatics is a novel interdisciplinary subject that involves the various processes of biological information by combining life sciences with computer technologies [33]. It is a great method to analyze complex biological data and understand the biological networks and regulatory mechanisms in theory. To date, numerous studies have been performed to uncover the roles of differential expression genes (DEGs) and identify many new biomarkers by using the aforementioned technologies in the corresponding diseases, including cancer. In KIRC, we screen many DEGs, identify various biomarkers, and construct the correlated prognostic risk models applying the methods to evaluate the status of patients from different aspects and elucidate the corresponding pathological mechanisms. Based on the research direction, the associated DEGs, markers, and models could be divided into the following types: tumor stage-related [34], immune-related [35–37], epigenetic-related [38–40], programmed cell death-related [41–43], drug-related [44,45], pathway-related [46,47], gene mutation-related [48], miRNA-related [49,50], lncRNA-related [51,52], etc. Therefore, it is significant that we found the diagnostic and prognostic markers and constructed the biological effect models to evaluate the KIRC patients using bioinformatics methods.

In this study, we carried out the comprehensive coalition analysis of TAZ/YAP using the

bioinformatic methods to explore their co-regulatory mechanisms and screen new prognostic biomarkers in KIRC. Firstly, we combined GSE121689 with the GSE146354 database and identified the co-expressed DEGs. Secondly, we explored their shared regulatory network, constructed a protein-protein interaction (PPI) network, screened important modules, and identified the hub genes. Thirdly, we discussed the signaling pathways of the hub genes. Fourthly, the hub genes were verified in the samples of the human protein atlas (HPA), UALCAN, and gene expression profiling interactive analysis (GEPIA). Finally, we explored the diagnostic value of the candidate gene using receiver operating character (ROC) analysis and the relationship between the candidate gene and physical immunity using the tumor immune estimation resource (TIMER) database. Based on the results of the aforementioned analysis, we found that the DEGs, influenced by TAZ/YAP, took part in the common regulatory interaction networks (TGF-β signaling pathway and endocytosis) and identified an immune-related novel biomarker (FMR1) that was positively correlated with immune infiltration and patients' prognosis. This study may provide new insight into the understanding of molecular mechanisms and the clinical prognosis of KIRC.

2. Materials and methods

The detailed process of the research was exhibited in Figure 1. The dataset, software, and website of the study were shown in Table 1.

Table 1. The information of databases, software, and website.

Name	Source
Cytoscape v3.8.2	http://cytoscape.org/
GEO	https://www.ncbi.nlm.nih.gov/geo/
GEPIA	http://gepia.cancer-pku.cn/
GDC	https://portal.gdc.cancer.gov/
GSEA v4.1.0	https://www.gsea-msigdb.org/gsea/index.jsp
HPA	https://www.proteinatlas.org/
MSigDB	https://www.gsea-msigdb.org/gsea/msigdb/index.jsp
RStudio v4.1.0	https://www.r-project.org/
STRING	https://www.string-db.org/
SangerBox	http://www.sangerbox.com/
TIMER	https://cistrome.shinyapps.io/timer/
UCSC Xena	https://xenabrowser.net/
UALCAN	http://ualcan.path.uab.edu/

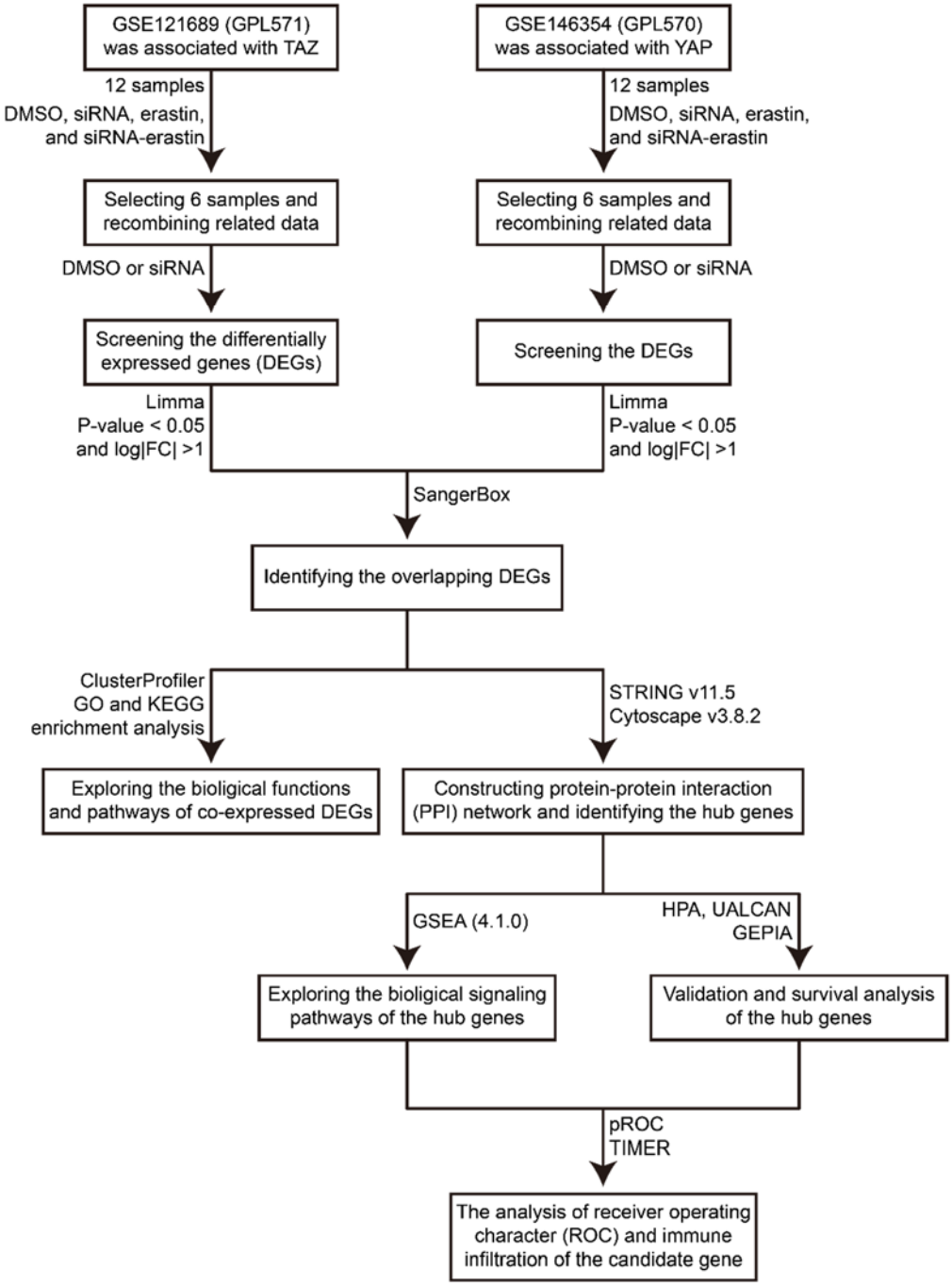

Figure 1. The analyzed flowchart of the research.

2.1. Selecting database and recombining microarray data

The gene expression omnibus (GEO) database is an international public repository that is easy to flexibly and freely obtain genomics data [53]. In this study, we downloaded the microarray datasets of GSE121689 (annotation information: Affymetrix human genome GPL571 platform) and GSE146354 (annotation information: Affymetrix human genome GPL570 platform) from GEO. GSE121689 was

associated with TAZ and had 12 samples that were treated with DMSO, siRNA, erastin, and siRNA-erastin, successively. GSE146354 was correlated with YAP and also had 12 samples that the processing method was the same as GSE121689. Here, we want to explore the co-regulatory mechanism of TAZ/YAP and identify novel biomarkers. According to our intention, we selected 12 samples that were handled with DMSO (as control) and siRNA in GSE121689 and GSE146354, respectively. Then, we recombined gene expression data for subsequent analysis.

2.2. Processing data and identifying co-expressed DEGs

The aforementioned microarray data was converted probe IDs to the corresponding gene symbols and was analyzed using RStudio v4.1.0. The Linear Models for Microarray data (limma) package was utilized to identify DEGs [54]. The filtered conditions were referenced in the related literature [55]. The results were saved as CSV text and were applied to draw volcano plots and heatmaps using packages of ggplot2 and pheatmap. Subsequently, the Venn diagram was drawn with SangerBox which was a simple visualization webpage tool to identify the overlapping genes.

2.3. Gene ontology (GO) and Kyoto encyclopedia of genes and genomes (KEGG) pathway enrichment analysis of DEGs

The clusterProfiler, an R package, was applied to execute GO and KEGG enrichment analyses to predict the functional roles of the co-expressed DEGs [56]. Among them, GO enrichment analyses consist of three aspects, which were described in the reference [57].

2.4. Constructing a PPI network and identifying the hub genes

To construct networks, the search tool for the retrieval of interacting genes (STRING) database was employed to analyze and predict the interactions of DEGs [58]. Cytoscape software v3.8.2 was applied to visualize the prediction network of DEGs proteins [59]. The threshold of the combined score was set as 0.4. The molecular complex detection (MCODE) and cytoHubba, plugins of Cytoscape, were used to filter the significant module and screen the nodes of the highest score and strongest connectivity to serve as the hub genes. The parameters of MCODE have referenced the related research [60].

2.5. Performing gene set enrichment analysis (GSEA) to identify the involved pathways of the hub genes

GSEA software v4.1.0 is applied to analyze the potential biological pathways of the different phenotypes based on statistically significant and concordant differences in RNA-seq profiles [61]. The KIRC expression profile (535 cancer samples) was downloaded from the UCSC Xena functional genomics explorer (UCSC Xena) and was separated into two groups according to the median level of the hub genes. Single-gene GSEA was executed to obtain their biological pathways by ranking the Spearman correlation coefficient of the hub gene and genes in the gene list. The selection of reference was the annotated genes set (c2.cp.kegg.v7.4.symbols.gmt) in Molecular Signatures Database (MSigDB). The threshold was set based on the related study [62].

2.6. Validation and OS and disease-free survival (DFS) analysis of the hub genes

The HPA is an opening database that is intended to map proteins in organs, tissues, and cells via various omics technologies [63]; UALCAN is a simply and conveniently online analyses tool to carry out the cancer genome atlas (TCGA) data mining [64]; while GEPIA is a formidable analysis website to perform some functions that are the analysis of gene expression, correlation, and survival based on the combination of TCGA database and genotype-tissue expression (GTEx) database [65]. In this research, immunohistochemistry images of the hub genes were obtained from HPA. The corresponding antibodies were CAB020836 (STAU2), HPA050118 (FMR1), and CAB019309 (AGO2). Their expressed data were obtained from the "expression" module and "KIRC" dataset of UALCAN. The "single gene analysis" module of GEPIA was used to execute the analyses of the pathological stage, OS, and DFS.

2.7. The ROC curves of the candidate genes

TCGA is an open-access database and collects a total of 33 cancer omics data, which is usually used by cancer-related researchers. Here, we downloaded the clinical data of KIRC from the genomic data commons (GDC). The collation of the data was executed by RStudio v4.1.0 to obtain a corresponding CSV text, which was analyzed and was visualized by the R packages of pROC and ggplot2, respectively. The area under the curve (AUC) of ROC represents the predicted accuracy of the candidate gene. The 0.5–1 of AUC is considered to predict sensitivity, which is divided into three degrees; including the low accuracy (0.5–0.7), the moderate accuracy (0.7–0.9), and the high accuracy (0.9–1) [66].

2.8. Immune cell infiltrates analysis of the candidate gene

TIMER is a webpage tool to systematically evaluate the relationships between gene and immune cell infiltration in diverse cancers [67]. In this research, the "Gene module" was applied to evaluate the relation between FMR1 and immune cells infiltration; the "SCNA module" was employed to assess the correlation between FMR1 mutation and immune cells infiltration; the "survival module" was utilized to explore the relationships between clinical outcomes and immune infiltrates or FMR1 expression; the "correlation module" was performed to identify the relevance between immune biomarkers and FMR1 expression.

2.9. Statistical analysis

All data was conducted in RStudio v4.1.0 and corresponding bioinformatic webpage tools. The statistical differences were calculated by Student's *t*-test, one-way analysis of variance (ANOVA), Spearman correlation analysis, cox regression analysis, and Kaplan-Meier analysis, respectively. The threshold was P-value < 0.05; $*P < 0.05$, $**P < 0.01$ and $***P < 0.001$.

3. Results

3.1. Choosing the DEGs and identifying the co-expressed DEGs based on GSE121689 and GSE146354

The data of GSE121689 and GSE146354 were normalized and analyzed using the limma package. We obtained a total of 165 DEGs (99 upregulated and 66 downregulated) in the GSE121689 dataset (Table S1); similarly, a total of 341 DEGs (117 upregulated and 224 downregulated) were selected in GSE146354 (Table S2). The volcano plots and heatmaps of DEGs were shown in Figure 2A–D. The Venn diagram was utilized to identify and visualize 51 overlapping DEGs (46 upregulated and 5 downregulated) that were shown in Figure 2E,F and Table S3, respectively.

3.2. GO and KEGG functional enrichment analysis of co-expressed DEGs

To comprehensively understand the biological functions and pathways of co-expressed DEGs, we executed the GO and KEGG analysis using clusterProfiler. The KEGG results indicated that the DEGs were significantly enriched in endocytosis and TGF-β signaling pathway (Figure 3A and Table S4). Meanwhile, the GO results mainly displayed the following three aspects: in the biological processes (BP) cluster, the enrichment terms were negative regulation of transport, signal release, negative regulation of secretion, endocrine process, regulation of receptor-mediated endocytosis, and negative regulation of exocytosis (Figure 3B and Table S4); while in the molecular functions (MF) cluster, the enrichment terms were receptor ligand activity, signaling receptor activator activity, hormone activity, growth factor activity, and structural molecule activity conferring elasticity (these functions were associated with the characteristics of TGF-β signaling pathway [68]) (Figure 3C and Table S4); in the cellular components (CC) cluster, the DEGs diversifications mainly focused on collagen-containing extracellular matrix and synapse components (asymmetric synapse, neuron to neuron synapse, presynapse, axon terminus, neuron projection terminus, distal axon, and postsynaptic density) (Figure 3D and Table S4). Subsequently, we also explored the interacting strength of signaling pathways of BP, MF, and CC, which found that there were different degrees of connection of the aforementioned pathways (Figure 3E–G). The aforementioned results concluded that the DEGs had enormous potential to regulate the activity of endocytosis and TGF-β signaling pathway to control the cellular procession.

3.3. Constructing a PPI network and identifying the hub genes

To intuitively understand and explore the interactive relationships of co-expressed DEGs, we performed the PPI network analyses using the STRING database and Cytoscape software. In this network, there were 14 nodes and 11 edges; 14 DEGs exhibited the interaction, including 10 upregulated genes (SLC4A8, STAU2, FMR1, CPEB3, DESI2, DENND5B, MFSD6, CSGALNACT2, ACT, and CFH) and 4 downregulated genes (NUPL1, AGO2, INHBE, and ADM) (Figure 4A). Then, the CytoHubba and MCODE of Cytoscape plugins were employed to confirm the hub genes; in the CytoHubba module, there were six genes which were AGO2, FMR1, STAU2, CPEB3, ADM, and MFSD6 (Figure 4B); in the MCODE module, there were three genes which were STAU2, FMR1, and AGO2 (Figure 4C). Finally, we found that the hub genes were STAU2, FMR1, and AGO2 according to the exhibition of the Venn diagram (Figure 4D and Table 2).

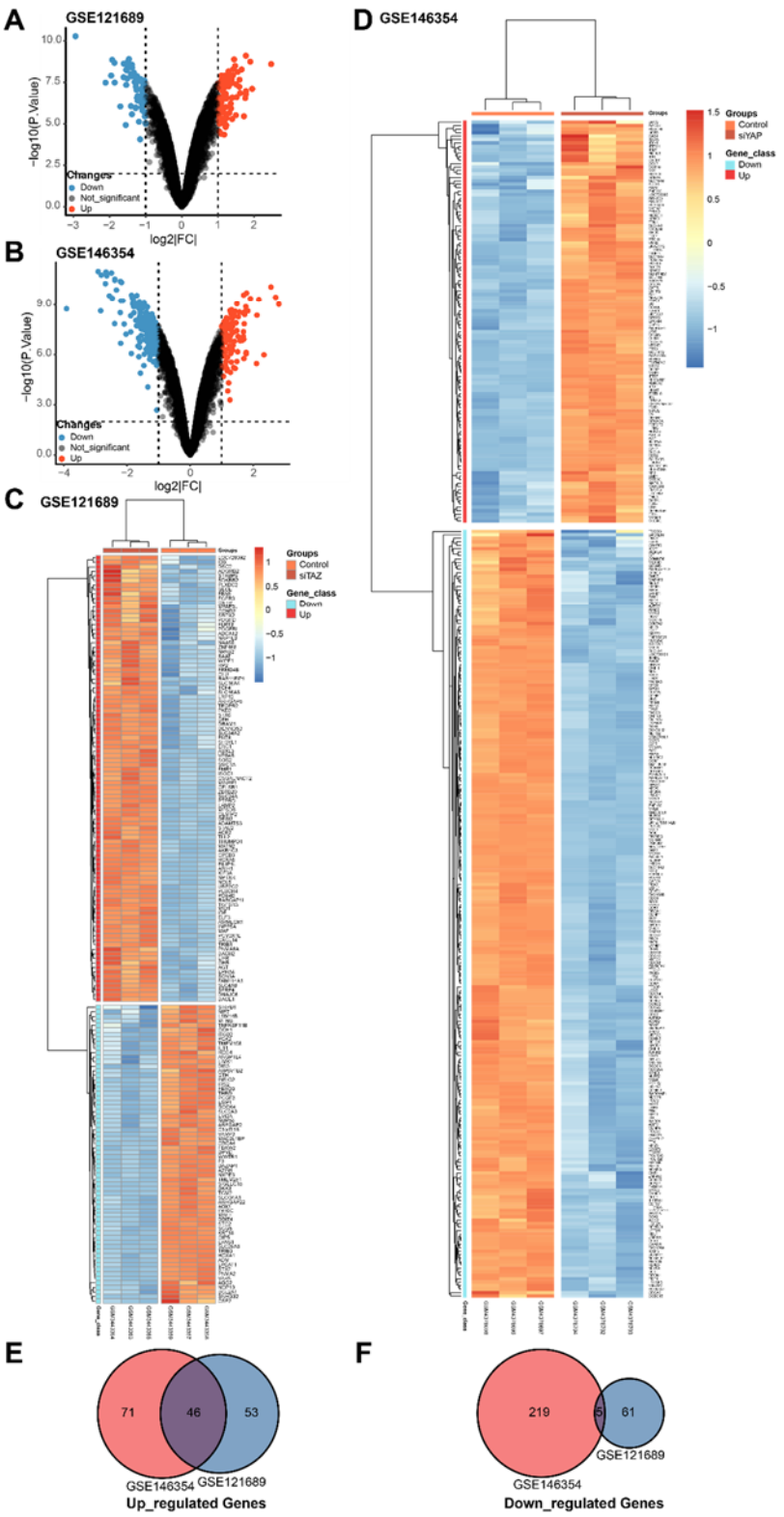

Figure 2. Identification of overlapping DEGs in the GSE121689 and GSE146354 database. (A,B) The volcano plots of DEGs; the upregulated genes and downregulated genes were shown in red and blue, respectively. (C,D) The heatmap of DEGs. (E,F) The Venn plots of overlapping upregulated and downregulated genes in two datasets, respectively. Log |fold change (FC)| > 1 and $*P < 0.05$.

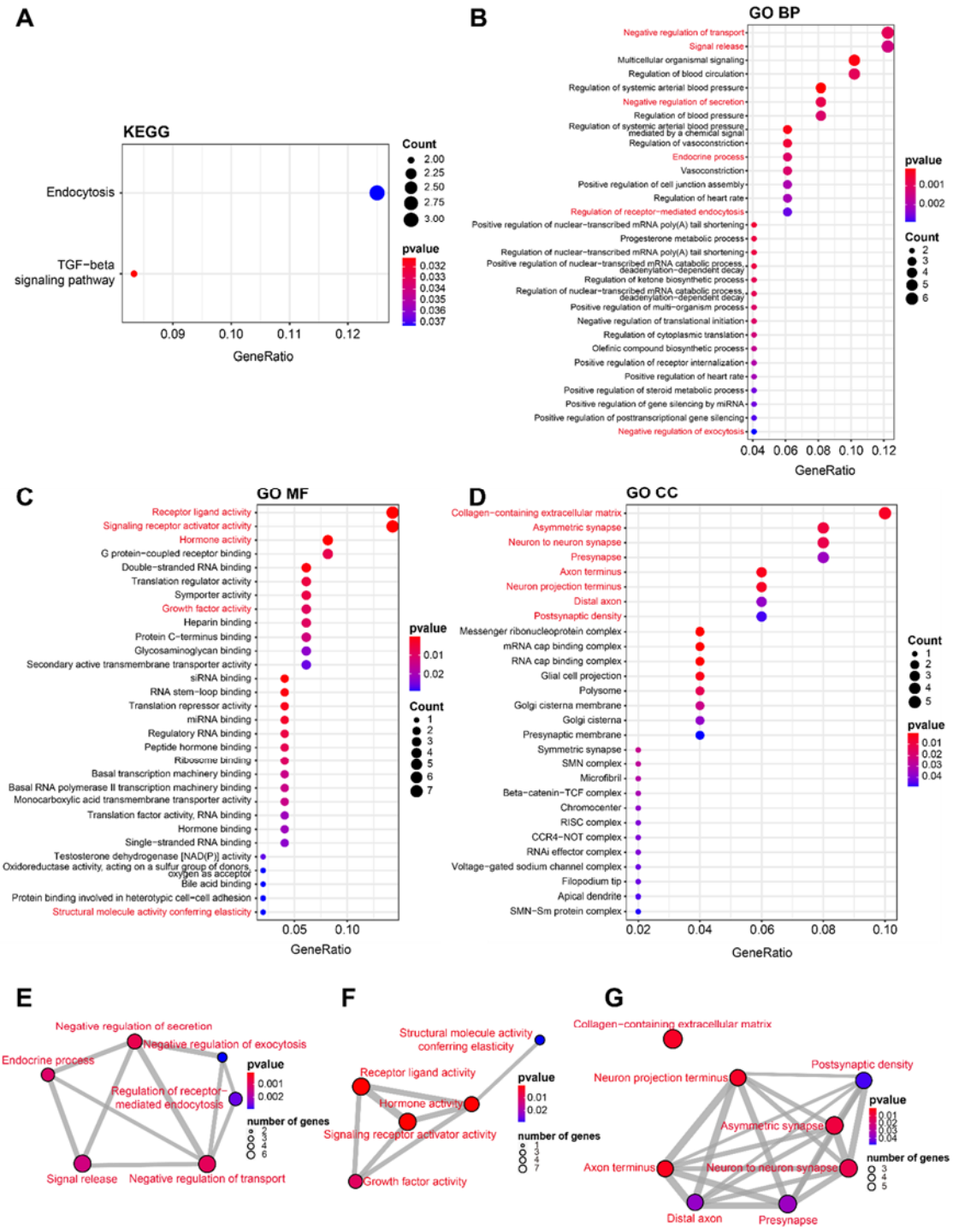

Figure 3. GO and KEGG analysis results of 51 co-expressed DEGs. (A) The KEGG results of the DEGs. (B) The GO BP results of the DEGs. (C) The GO MF results of the DEGs. (D) The GO CC results of the DEGs. (E–G) The interaction of pathways of BP, MF, and CC; the degrees of the line-thickness represented the interacting strength of pathways. *$P < 0.05$.

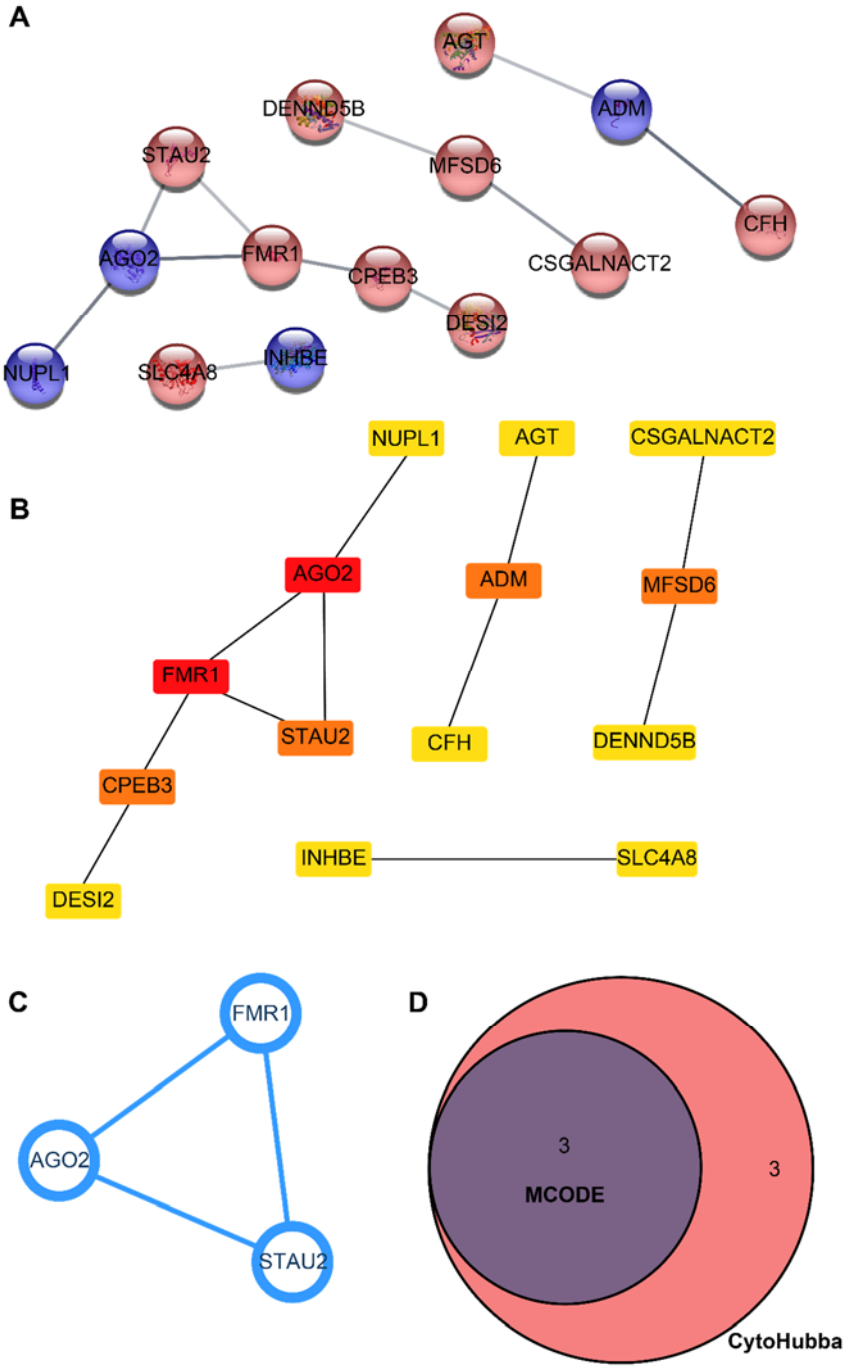

Figure 4. The PPI network of co-expressed DEGs and the confirmation of hub genes. (A) The PPI network of 14 DEGs; red nodes are upregulated genes, whereas blue nodes are downregulated genes. (B) The top six genes were filtered by CytoHubba; the variational colors of nodes represent the different statistical significance. Red is the highest significance, orange is the middle significance, and yellow is the lowest significance. (C) The significant module was identified by MCODE, including three genes. (D) The Venn diagram was applied to screen the hub genes in MCODE and CytoHubba.

Table 2. The Venn analysis results of the MCODE and CytoHubba.

Names	Total	Elements	Common Elements
MCODE	3	STAU2, FMR1, AGO2	STAU2, AGO2, FMR1
CytoHubba	6	CPEB3, FMR1, AGO2, STAU2, ADM, MFSD6	

3.4. The biological signaling pathways of the hub genes

To further elucidate the biological networks and pathways of the aforementioned hub genes in KIRC, we executed a KEGG analysis using GSEA. The results indicated that the hub genes were associated with metabolic pathways (ubiquitin-mediated proteolysis, lysosome, endocytosis, valine leucine and isoleucine degradation, and peroxisome) and physical immune system (allograft rejection, graft versus host disease, systemic lupus erythematosus, primary immunodeficiency, intestinal immune network for IGA production, B cell receptor signaling pathway, T cell receptor signaling pathway, and Toll-like receptor signaling pathway) (Figure 5A–C). Based on enriched similar functional terms, we found that the overexpression of STAU2 and AGO2 made the active states of ubiquitin-mediated proteolysis and endocytosis (Figure 5A,B), while AGO2 and FMR1 enhanced the immune system activity to probably cause immune function disorder in the high expression groups (Figure 5B,C). In conclusion, the abovementioned results demonstrated that the three genes and their expression-related genes had affected physical functions by regulating the procession of metabolism and immune; especially, FMR1 paid high attention to the regulation of the immune system.

3.5. Validation and survival analysis of the hub genes to determine FMR1 as a candidate gene

To confirm the reliable roles of the hub genes in KIRC development, the datasets of HPA, UALCAN, and GEPIA were utilized to explore the relationships between expressional changes of the hub genes and the prognosis and clinical outcomes of the patients. The immunohistochemical results of the hub genes in the HPA database showed that STAU2 and FMR1 were high-expressed in the cytoplasm and membrane of normal kidney cells, while STAU2 and FMR1 were weakly expressed in the nucleus and cytoplasm/membrane of tumor cells, respectively (Figure 6A,B). However, the expression level of AGO2 was unchanged in the cytoplasm and membrane of normal and KIRC tissues (Figure 6C). Similarly, the UALCAN boxplot results indicated that STAU2 and FMR1 were significantly downregulated in the tumor, whereas AGO2 variation was not statistically significant (Figure 7A). Meanwhile, we found that STAU2 and FMR1 were negatively associated with KIRC stages (Figure 7B). Subsequently, we also performed the Kaplan-Meier curve and log-rank test analyses to exhibit the correlation between the hub genes (STAU2, FMR1, and AGO2) and OS and DFS of patients. The results showed that only FMR1 was meaningful for patients' OS and DFS. The deregulated FMR1 was correlated with poor OS and DFS (Figure 7C,D). FMR1 may be served as an anti-oncogene.

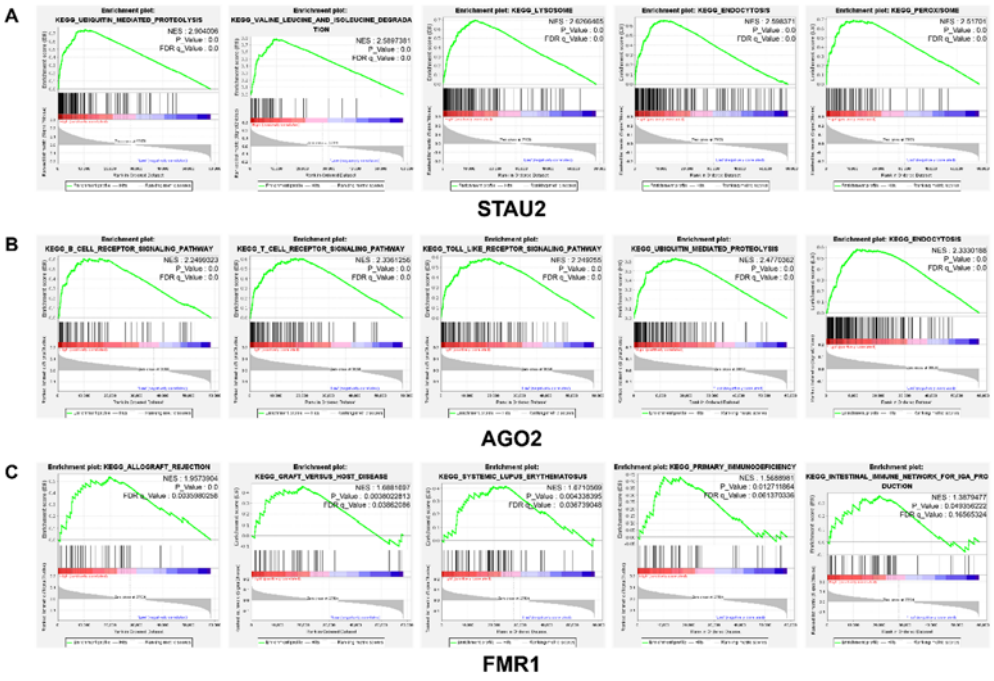

Figure 5. The KEGG-related pathways of three hub genes. (A) The GSEA results of STAU2. (B) The GSEA results of AGO2. (C) The GSEA results of FMR1. |NES| > 1, NOM *P-value < 0.05, and FDR q-value < 0.25.

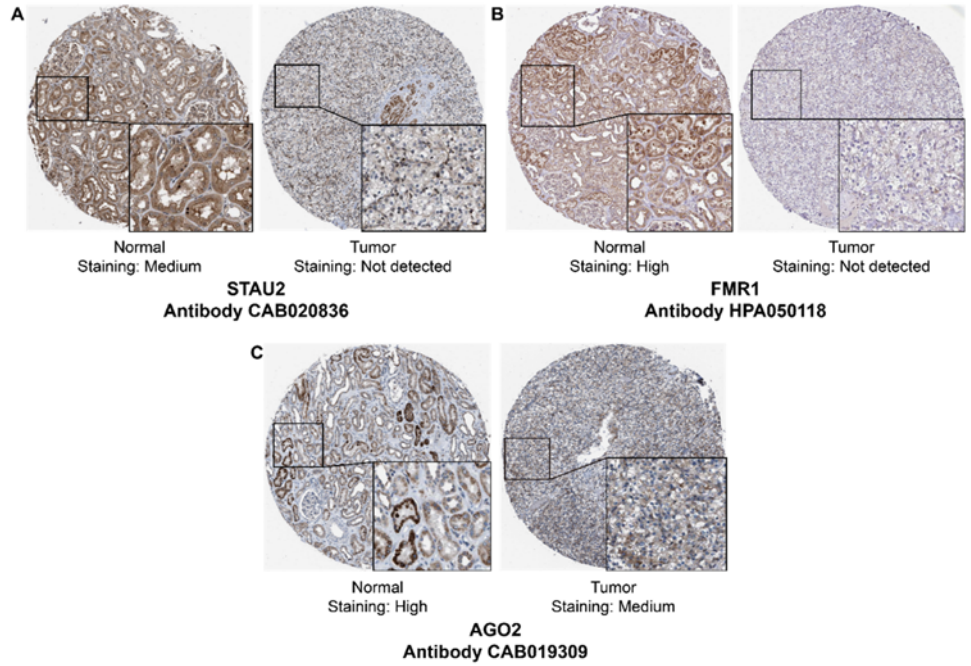

Figure 6. The expressions of the hub genes were verified by the HPA database in KIRC. (A) The immunohistochemistry images of STAU2. (B) The immunohistochemistry images of FMR1. (C) The immunohistochemistry images of AGO2.

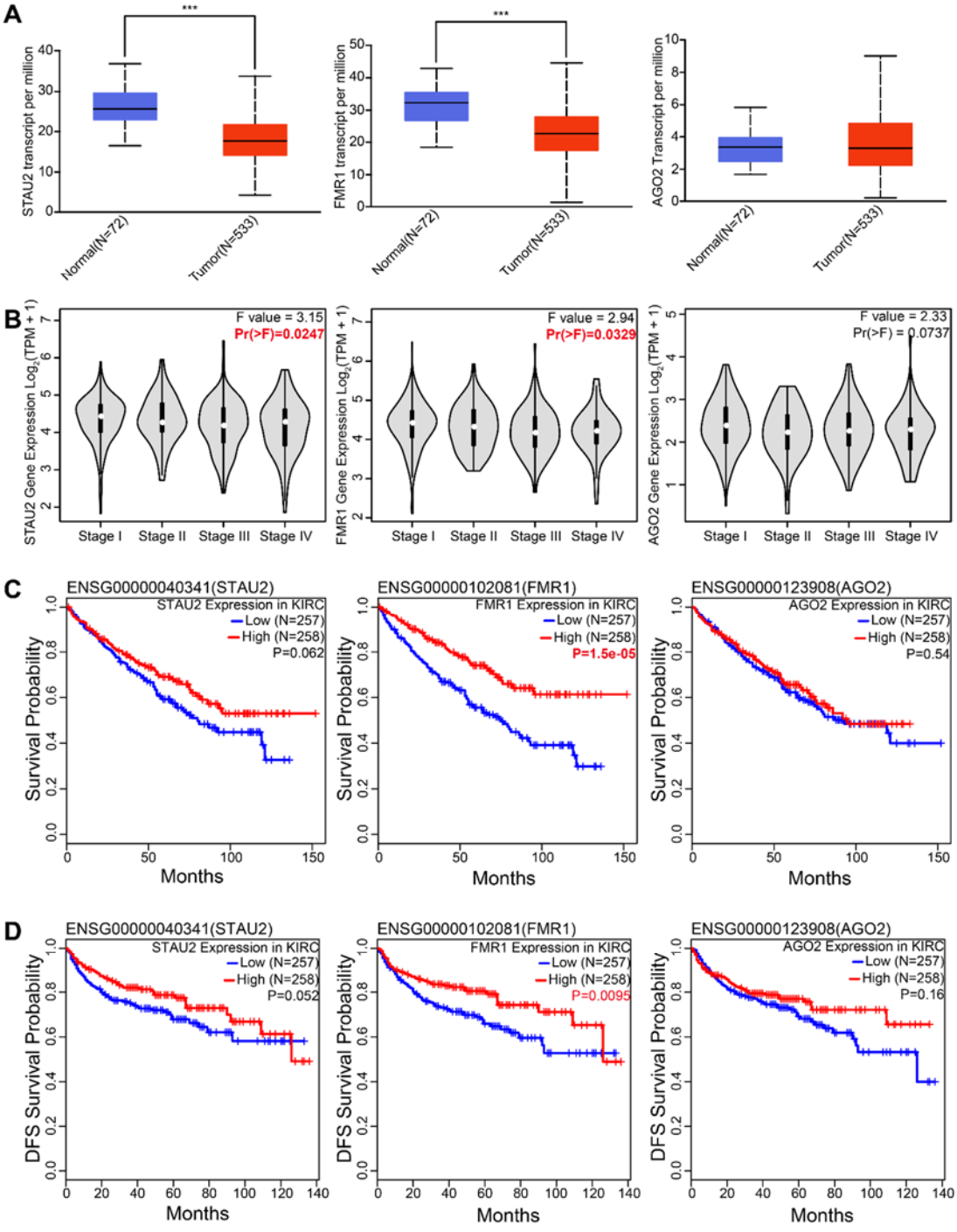

Figure 7. The relationships between three hub genes and clinical characteristics and prognostic outcomes of KIRC patients. (A) The differential expression of STAU2, FMR1, and AGO2 between adjacent normal tissues and tumor tissues. (B) The clinical stages of STAU2, FMR1, and AGO2. (C) The OS curves of STAU2, FMR1, and AGO2. (D) The DFS curves of STAU2, FMR1, and AGO2. *$P < 0.05$, **$P < 0.01$, and ***$P < 0.001$.

3.6. The ROC curves of FMR1

To identify the diagnostic value of FMR1 in distinguishing KIRC patients from the normal, we executed the ROC analysis using pROC. The result showed that the AUC of FMR1 was 0.645 and the confidence interval (CI) was 0.59–0.7 (Figure 8), which implied that FMR1 had a certain predictive ability.

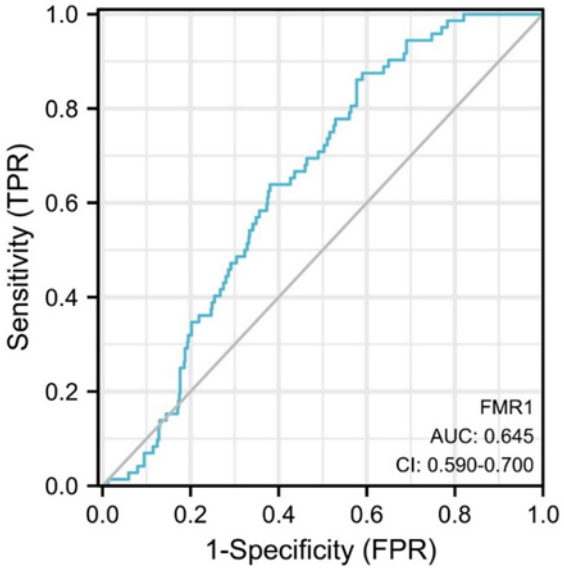

Figure 8. The ROC analysis of FMR1 (normal vs tumor).

3.7. FMR1 serves as an immune-related gene in KIRC

Based on the above-mentioned GSEA and prognosis analysis results, FMR1 was probably a potential prognostic biomarker and had a strong influence on immunomodulation in KIRC. Therefore, we performed the co-expressed analysis to explore the relationship between FMR1 and immune cell infiltration using TIMER. The results demonstrated that FMR1 was positively correlated with the B cells (cor = 0.241, P = 1.77e-07), $CD8^+$ T cells (cor = 0.135, P = 4.69e-03), $CD4^+$ T cells (cor = 0.356, P = 3.59e-15), macrophages (cor = 0.437, P = 2.41e-22), neutrophils (cor = 0.395, P = 1.64e-18) and dendritic cells (DCs, cor = 0.256, P = 3.18e-08) (Figure 9A). In 57 immune cell biomarkers, FMR1 had co-expressed relationships with 33 immune markers, including 27 positive correlations and 6 negative relations (Figure 9D and Table S5). Moreover, we found that FMR1 mutation negatively regulated immune cell infiltration (Figure 9B). The low expression of $CD8^+$ T cells, macrophages, and FMR1 were correlated with poor prognosis through survival analysis (Figure 9C). In addition to the above analysis, we also selected more than 40 common immune checkpoint genes to perform the co-expressed analysis. The results indicated that there were 31 co-expressed connections, including 23 positive correlations and 8 negative correlations (Figure 9E). Some research revealed that the chemokine-chemokine receptor interactions promoted the immune cells' enrichment of the tumor microenvironment to influence tumor development [69]. Subsequently, we discussed the co-expressed relationships between FMR1 and chemokines or chemokine receptors. The results exhibited that FMR1 was associated with the expression of the chemokines (21, 11 positive correlations and 10 negative correlations) (Figure 9F) and commonly positively correlated with the chemokine receptors' expression (14, 12 positive correlations and 2

negatively correlations) (Figure 9G). In summary, FMR1 plays a vital role in immune infiltration to affect the KIRC progression and is a potential immune-related prognostic gene.

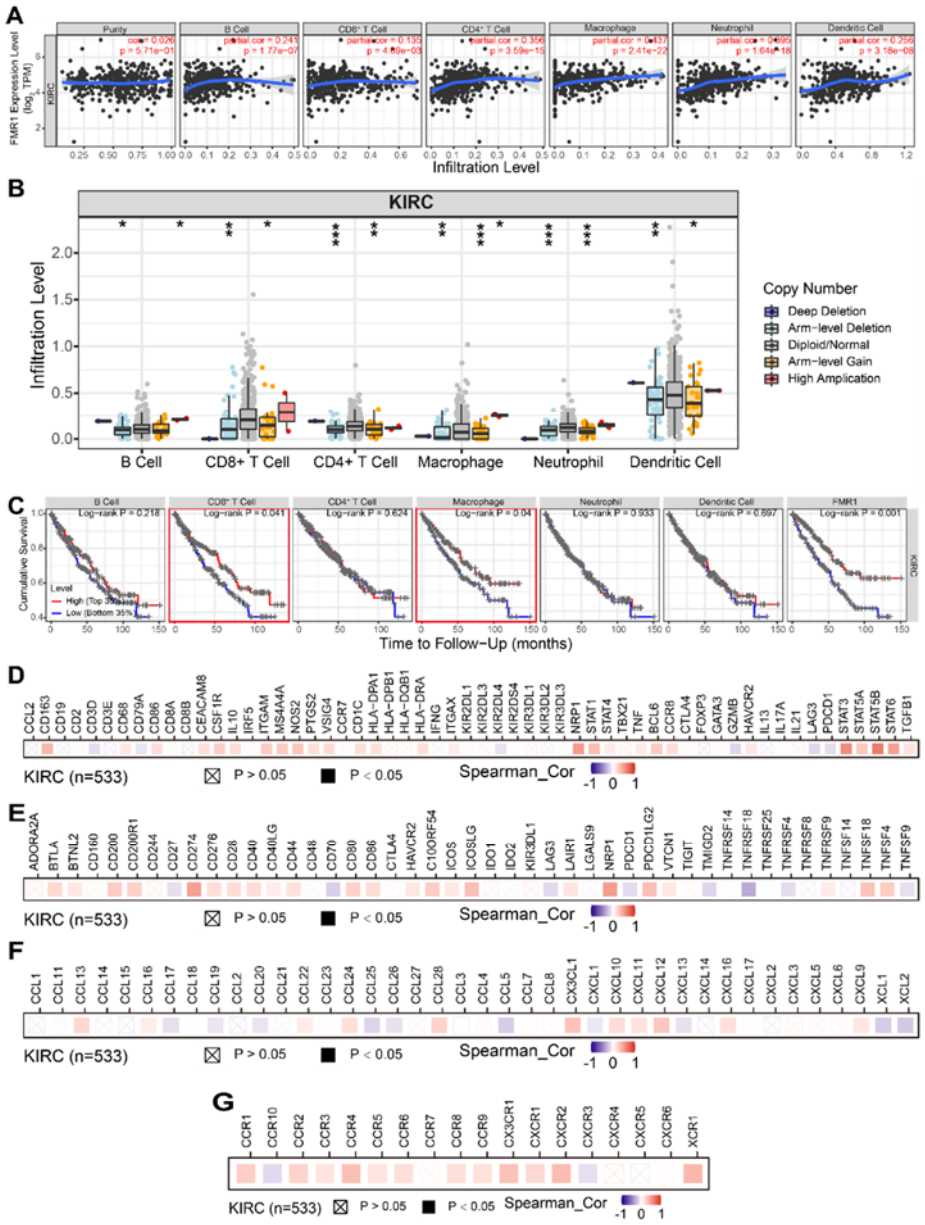

Figure 9. Immunological analysis of FMR1. (A) The association between FMR1 and immune cell infiltration. (B) The relation between FMR1 mutation and immune cell infiltration. (C) The survival analysis of FMR1 and immune cells. (D) The heatmap of co-expressed analysis of FMR1 and immune cells biomarkers. (E) The heatmap of co-expressed analysis of FMR1 and immunological checkpoint genes. (F) The heatmap of co-expressed analysis of FMR1 and chemokines-related genes. (G) The heatmap of co-expressed analysis of FMR1 and chemokine receptors related genes. $*P < 0.05$, $**P < 0.01$, and $***P < 0.001$.

4. Discussion

TAZ/YAP is the most common oncogenes in various cancers; while there are double functions of TAZ/YAP in RCC, including the promotor and inhibitor of cancer. Mechanically, the overwhelming research indicated that TAZ/YAP promoted cell proliferation, migration, and invasion to influence the process of cancer [70,71]. Furthermore, TAZ and YAP could regulate the expression of the related immune molecule (programmed cell death ligand 1 (PDL1) [72]) or related angiogenic growth factor (vascular endothelial growth factors A (VEGFA) [73]), respectively; thereby creating a suitable microenvironment for the aforementioned pathological process. It is indubitable that the nuclear accumulation of TAZ/YAP did contribute to the formation of the aggressive RCC [74]. Interestingly, some studies demonstrated that TAZ/YAP prevented the above-mentioned functions by regulating F-actin, P53, apoptosis, and ferroptosis [27,29,75,76]. While a combined TAZ/YAP analysis revealed that they influenced the cell metabolism process to promote the RCC development of NF2 mutation [32]. However, there isn't a combined analysis of TAZ/YAP to explore their common regulatory mechanisms in mutation-free RCC, especially in KIRC.

Bioinformatics essentially is an analyzed method that uses related computer technology to process genomics data. It theoretically can screen the diagnostic and prognostic biomarkers and explain the corresponding mechanism of diseases, which is convenient for developing effective diagnosis and treatment measures. Recently, emerging scholars have paid attention to the development of the related analytical tools with more effective and accurate, so that the analytical methods have become more diverse and simpler. Presently, the R packages of limma [54], edgeR [77], and DESeq2 [78,79] were the common methods to screen DEGs; the webpage tools of DAVID [80], KOBAS [81], Metascape [82], and WebGestalt [83] could be applied to enrichment analysis to obtain the corresponding signaling pathways; the tools of STRING [58], LncBase [84], miRTarBase [85], Starbase [86], and Cytoscape [59] were used to predict and construct the interaction of gene-gene; and the associated computational models (IMBDANET [87], lncRNA–miRNA association prediction (NDALMA) [88], logistic matrix factorization with neighborhood regularized (LMFNRLMI) [89], deep forest ensemble learning based on autoencoder (DFELMDA) [90], and the computational models of predicted circRNA-diseases [91]) were proposed to predict the correlation between gene and gene or diseases. These methods revealed the related regulatory networks and the corresponding molecular mechanisms form different aspects, which made us have comprehensive understanded to the pathological process of diseases. Some above-analyzed results have confirmed by the relevant experiments [92–94], which verified the accuracy of the bioinformatic results.

In our study, we performed the comprehensive conjoint analysis of TAZ/YAP utilizing bioinformatic methods to reveal their co-regulatory mechanisms and identify new prognostic biomarkers in KIRC. Here, we identified 51 co-expressed DEGs and three hub genes (STAU2, FMR1, and AGO2), but only FMR1 was consistent with the clinical characteristics and prognosis outcomes of patients. The KEGG terms of the co-expressed DEGs were TGF-β signaling pathway and endocytosis, which was supported by the GO results. Research indicated that the TGF-β signaling pathway took part in the regulation of complicated mechanical signal networks and exhibited double functions (tumor-suppressing and tumor-promoting) to maintain physical homeostasis or promote tumor development by influencing cell proliferation, migration, invasion, drug resistance, and tumor escape [95]; while endocytosis was an internalized process that involved in absorbing nutrients, signaling proteins, and other cargoes, which were correlated with cellular metabolism. This study

showed that TAZ/YAP commonly regulated TGF-β signaling pathway and endocytosis to control cellular procession in KIRC.

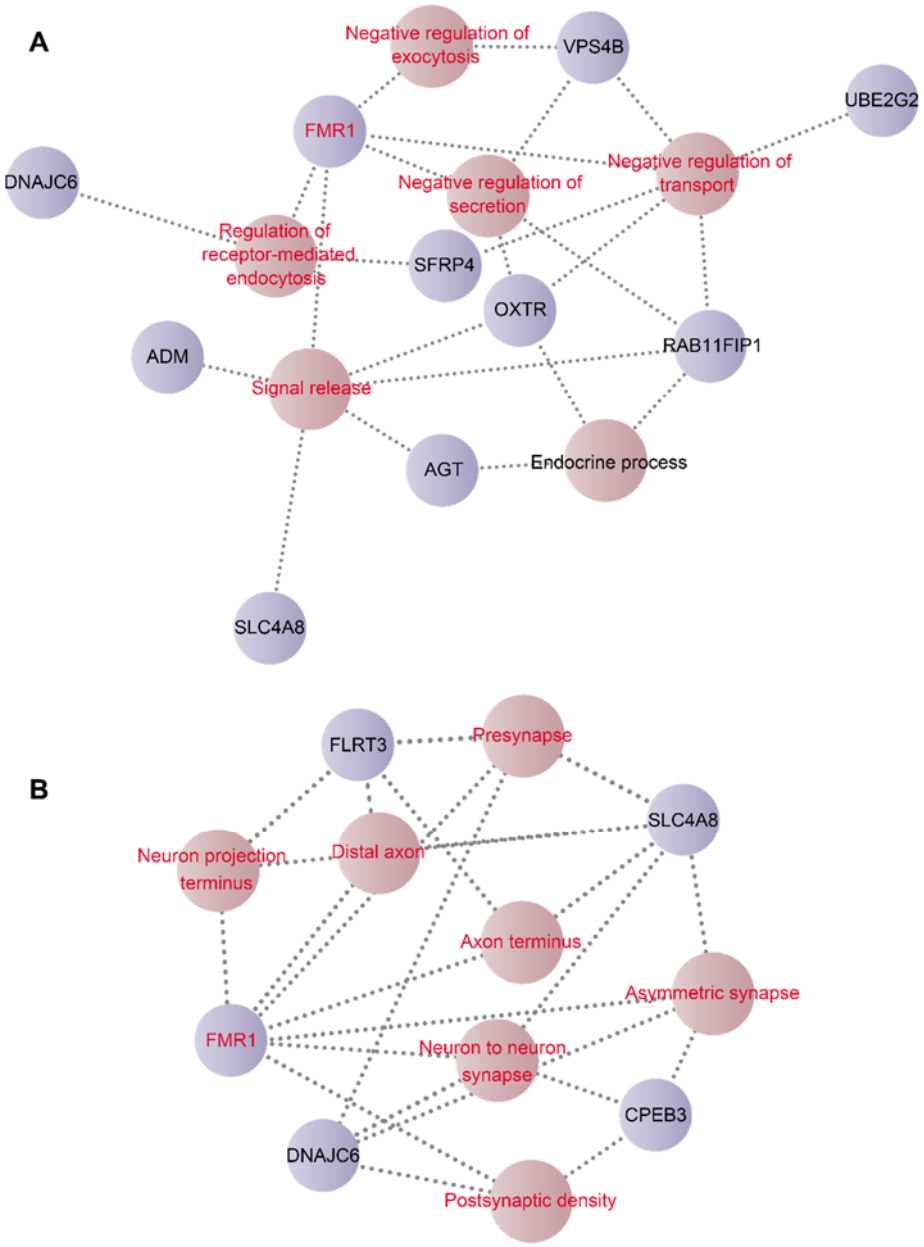

Figure 10. The connection between the pathways and genes in GO enrichment pathways. (A) The relation between the BP pathways and genes. (B) The association between the CC pathways and genes.

FMR1 is a multifunctional polyribosome-associated RNA-binding protein that is involved in RNA maturity and stability [96]. Its epigenetic transformation is tightly associated with the progression of cancers [97–100], neurodegenerative disorders, and immunomodulation dysfunctions [101–103]. In GO results, FMR1 was involved in some GO pathways, including the negative regulation of transport, signal release, negative regulation of secretion, regulation of receptor−mediated endocytosis,

negative regulation of exocytosis, and synapse components (Figure 10A,B and Table S4); which indicated that this gene was closely associated with the regulation of neuroendocrine functions and the development of the nervous system. In addition, some research showed that FMR1 created an abnormal immune microenvironment by affecting the production of cytokines (IL-β, IL-6, TNF-α, and IL-10) [104,105] and the surface biomarkers activity of immune cells (T cells) [103], which was consistent with its GSEA results. Therefore, we performed the co-expressed analysis of this gene and immune cells, immune checkpoints, chemokines, and chemokine receptors. We found that the gene was closely correlated with the aforementioned biomarkers. Meanwhile, we also found that FMR1 was significantly deregulated in KIRC tissue and exhibited a negative relationship with the stage of patients; the poor prognosis was associated with its weak expression; the ROC result indicated that FMR1 owned a certain predictive sensibility to distinguish KIRC patients from the normal. These results implied that FMR1 could be served as a tumor suppressor gene and a potential novel immune-related prognostic molecule in KIRC, which provided a new target and theoretical basis for the KIRC treatment strategy. Although the above conclusions were confirmed by the public databases, more experiments are still needed for further analysis and validation.

5. Conclusions

In conclusion, TAZ/YAP had influenced 51 common DEGs to take part in the regulation of TGF-β signaling pathway and endocytosis, thereby controlling the KIRC development procession. Even though we identified three hub genes (STAU2, FMR1, and AGO2), only FMR1 was consistent with the clinical characteristics and prognosis outcomes of the patients. We found that FMR1 was downregulated in KIRC tissues, exhibited an unfavorable prognosis, and had a certain predictive sensibility to distinguish KIRC patients from the normal. Meanwhile, FMR1 was tightly associated with immunomodulation. The prementioned results implied that FMR1 could be served as an antitumor gene and was a potential novel immune-related prognostic molecule in KIRC.

Acknowledgments

This work was supported by the National Natural Science Foundation of China (81802785 [Y. Jiang]), Hunan Provincial Natural Science Foundation of China (2020JJ5382 [Y. Jiang], 2020JJ8051 [J. Huang]), Scientific Research Program of Hunan Provincial Health Commission (202202065445 [Y. Jiang]). We sincerely thank Ph.D. Chanjuan Zheng for her suggestions in this research. We thank all participants.

Conflict of interest

The authors declare that there are no potential conflicts of interest.

References

1. Y. Wang, Y. Zhang, P. Wang, X. Fu, W. Lin, Circular RNAs in renal cell carcinoma: implications for tumorigenesis, diagnosis, and therapy, *Mol. Cancer*, **19** (2020), 149. https://doi.org/10.1186/s12943-020-01266-7

2. H. Sung, J. Ferlay, R. L. Siegel, M. Laversanne, I. Soerjomataram, A. Jemal, et al., Global cancer statistics 2020: GLOBOCAN estimates of incidence and mortality worldwide for 36 cancers in 185 countries, *CA Cancer J. Clin.*, **71** (2021), 209–249. https://doi.org/10.3322/caac.21660
3. M. He, F. Hu, TF-RBP-AS Triplet analysis reveals the mechanisms of aberrant alternative splicing events in kidney cancer: implications for their possible clinical use as prognostic and therapeutic biomarkers, *Int. J. Mol. Sci.*, **22** (2021), 8789. https://doi.org/10.3390/ijms22168789
4. A. Znaor, J. Lortet-Tieulent, M. Laversanne, A. Jemal, F. Bray, International variations and trends in renal cell carcinoma incidence and mortality, *Eur. Urol.*, **67** (2015), 519–530. https://doi.org/10.1016/j.eururo.2014.10.002
5. Z. Sun, C. Jing, X. Guo, M. Zhang, F. Kong, Z. Wang, et al., Comprehensive analysis of the immune infiltrates of pyroptosis in kidney renal clear cell carcinoma, *Front. Oncol.*, **11** (2021), 716854. https://doi.org/10.3389/fonc.2021.716854
6. X. Mao, J. Xu, W. Wang, C. Liang, J. Hua, J. Liu, et al., Crosstalk between cancer-associated fibroblasts and immune cells in the tumor microenvironment: new findings and future perspectives, *Mol. Cancer*, **20** (2021), 131. https://doi.org/10.1186/s12943-021-01428-1
7. L. F. S. Patterson, S. A. Vardhana, Metabolic regulation of the cancer-immunity cycle, *Trends Immunol.*, **42** (2021), 975–993. https://doi.org/10.1016/j.it.2021.09.002
8. Y. Senbabaoglu, R. S. Gejman, A. G. Winer, M. Liu, E. M. Van Allen, G. de Velasco, et al., Tumor immune microenvironment characterization in clear cell renal cell carcinoma identifies prognostic and immunotherapeutically relevant messenger RNA signatures, *Genome Biol.*, **17** (2016), 231. https://doi.org/10.1186/s13059-016-1092-z
9. B. Wang, D. Chen, H. Hua, TBC1D3 family is a prognostic biomarker and correlates with immune infiltration in kidney renal clear cell carcinoma, *Mol. Ther. Oncolytics*, **22** (2021), 528–538. https://doi.org/10.1016/j.omto.2021.06.014
10. G. Liao, P. Wang, Y. Wang, Identification of the prognosis value and potential mechanism of immune checkpoints in renal clear cell carcinoma microenvironment, *Front. Oncol.*, **11** (2021), 720125. https://doi.org/10.3389/fonc.2021.720125
11. A. D. Janiszewska, S. Poletajew, A. Wasiutyński, Reviews Spontaneous regression of renal cell carcinoma, *Współczesna Onkologia*, **2** (2013), 123–127. https://doi.org/10.5114/wo.2013.34613
12. B. A. Inman, M. R. Harrison, D. J. George, Novel immunotherapeutic strategies in development for renal cell carcinoma, *Eur, Urol,*, **63** (2013), 881–889. https://doi.org/10.1016/j.eururo.2012.10.006
13. A. Kulkarni, M. T. Chang, J. H. A. Vissers, A. Dey, K. F. Harvey, The Hippo pathway as a driver of select human cancers, *Trends Cancer*, **6** (2020), 781–796. https://doi.org/10.1016/j.trecan.2020.04.004
14. Y. Zheng, D. Pan, The hippo signaling pathway in development and disease, *Dev. Cell*, **50** (2019), 264–282. https://doi.org/10.1016/j.devcel.2019.06.003
15. M. Moloudizargari, M. H. Asghari, S. F. Nabavi, D. Gulei, I. Berindan-Neagoe, A. Bishayee, et al., Targeting Hippo signaling pathway by phytochemicals in cancer therapy, *Semin. Cancer Biol.*, **80** (2020), 183–194. https://doi.org/10.1016/j.semcancer.2020.05.005
16. F. Reggiani, G. Gobbi, A. Ciarrocchi, V. Sancisi, YAP and TAZ are not identical twins, *Trends Biochem. Sci.*, **46** (2021), 154–168. https://doi.org/10.1016/j.tibs.2020.08.012
17. H. Zhang, C. Y. Liu, Z. Y. Zha, B. Zhao, J. Yao, S. Zhao, et al., TEAD transcription factors mediate the function of TAZ in cell growth and epithelial-mesenchymal transition, *J. Biol. Chem.*, **284** (2009), 13355–13362. https://doi.org/10.1074/jbc.M900843200
18. B. Zhao, X. Ye, J. Yu, L. Li, W. Li, S. Li, et al., TEAD mediates YAP-dependent gene induction and growth control, *Genes Dev.*, **22** (2008), 1962–1971. https://doi.org/10.1101/gad.1664408

19. M. Murakami, J. Tominaga, R. Makita, Y. Uchijima, Y. Kurihara, O. Nakagawa, et al., Transcriptional activity of Pax3 is co-activated by TAZ, *Biochem. Biophys. Res. Commun.*, **339** (2006), 533–539. https://doi.org/10.1016/j.bbrc.2005.10.214
20. Z. Miskolczi, M. P. Smith, E. J. Rowling, J. Ferguson, J. Barriuso, C. Wellbrock, et al., Collagen abundance controls melanoma phenotypes through lineage-specific microenvironment sensing, *Oncogene*, **37** (2018), 3166–3182. https://doi.org/10.1038/s41388-018-0209-0
21. M. Murakami, M. Nakagawa, E. Olson, O. Nakagawa, A WW domain protein TAZ is a critical coactivator for TBX5 a transcription factor implicated in Holt Oram syndrome, *Proc. Natl. Acad. Sci.*, **102** (2005), 18034–18039. https://doi.org/10.1073/pnas.0509109102
22. J. Rosenbluh, D. Nijhawan, A. G. Cox, X. Li, J. T. Neal, E. J. Schafer, et al., beta-Catenin-driven cancers require a YAP1 transcriptional complex for survival and tumorigenesis, *Cell*, **151** (2012), 1457–1473. https://doi.org/10.1016/j.cell.2012.11.026
23. F. Zanconato, M. Forcato, G. Battilana, L. Azzolin, E. Quaranta, B. Bodega, et al., Genome-wide association between YAP/TAZ/TEAD and AP-1 at enhancers drives oncogenic growth, *Nat. Cell Biol.*, **17** (2015), 1218–1227. https://doi.org/10.1038/ncb3216
24. H. L. Li, Q. Y. Li, M. J. Jin, C. F. Lu, Z. Y. Mu, W. Y. Xu, et al., A review: hippo signaling pathway promotes tumor invasion and metastasis by regulating target gene expression, *J. Cancer Res. Clin. Oncol.*, **147** (2021), 1569–1585. https://doi.org/10.1007/s00432-021-03604-8
25. G. D. Chiara, F. Gervasoni, M. Fakiola, C. Godano, C. D'Oria, L. Azzolin, et al., Epigenomic landscape of human colorectal cancer unveils an aberrant core of pan-cancer enhancers orchestrated by YAP/TAZ, *Nat. Commun.*, **12** (2021), 2340. https://doi.org/10.1038/s41467-021-22544-y
26. Y. Wang, X. Xu, D. Maglic, M. T. Dill, K. Mojumdar, P. K. S. Ng, et al., Comprehensive molecular characterization of the hippo signaling pathway in cancer, *Cell Rep.*, **25** (2018), 1304–1317. https://doi.org/10.1016/j.celrep.2018.10.001
27. W. H. Yang, C. K. C. Ding, T. Sun, G. Rupprecht, C. C. Lin, D. Hsu, et al., The hippo pathway effector taz regulates ferroptosis in renal cell carcinoma, *Cell Rep.*, **28** (2019), 2501–2508. https://doi.org/10.1016/j.celrep.2019.07.107
28. W. H. Yang, Z. Huang, J. Wu, C. K. C. Ding, S. K. Murphy, J. T. Chi, A TAZ-ANGPTL4-NOX2 axis regulates ferroptotic cell death and chemoresistance in epithelial ovarian cancer, *Mol. Cancer Res.*, **18** (2020), 79–90. https://doi.org/10.1158/1541-7786.MCR-19-0691
29. W. H. Yang, C. C. Lin, J. Wu, P. Y. Chao, K. Chen, P. H. Chen, et al., The hippo pathway effector YAP promotes ferroptosis via the E3 Ligase SKP2, *Mol. Cancer Res.*, **19** (2021), 1005–1014. https://doi.org/10.1158/1541-7786.MCR-20-0534
30. M. Pavel, M. Renna, S. J. Park, F. M. Menzies, T. Ricketts, J. Füllgrabe, et al., Contact inhibition controls cell survival and proliferation via YAP/TAZ-autophagy axis, *Nat. Commun.*, **9** (2018), 2961. https://doi.org/10.1038/s41467-018-05388-x
31. M. Toth, L. Wehling, L. Thiess, F. Rose, J. Schmitt, S. M. Weiler, et al., Co-expression of YAP and TAZ associates with chromosomal instability in human cholangiocarcinoma, *BMC Cancer*, **21** (2021), 1079. https://doi.org/10.1186/s12885-021-08794-5
32. S. M. White, M. L. Avantaggiati, I. Nemazanyy, C. Di Poto, Y. Yang, M. Pende, et al., YAP/TAZ inhibition induces metabolic and signaling rewiring resulting in targetable vulnerabilities in NF2-deficient tumor cells, *Dev. Cell*, **49** (2019), 425–443. https://doi.org/10.1016/j.devcel.2019.04.014
33. S. W. Zhang, N. Zhang, N. Wang, Role of COL3A1 and POSTN on pathologic stages of esophageal cancer, *Technol. Cancer Res. Treat.*, **19** (2020), 1533033820977489. https://doi.org/10.1177/1533033820977489

34. D. Xu, Y. Xu, Y. Lv, F. Wu, Y. Liu, M. Zhu, et al., Identification of four pathological stage-relevant genes in association with progression and prognosis in clear cell renal cell carcinoma by integrated bioinformatics analysis, *Biomed. Res. Int.*, **2020** (2020), 2137319. https://doi.org/10.1155/2020/2137319
35. S. Bai, L. Chen, Y. Yan, X. Wang, A. Jiang, R. Li, et al., Identification of hypoxia-immune-related gene signatures and construction of a prognostic model in kidney renal clear cell carcinoma, *Front. Cell Dev. Biol.*, **9** (2021), 796156. https://doi.org/10.3389/fcell.2021.796156
36. S. Sun, W. Mao, L. Wan, K. Pan, L. Deng, L. Zhang, et al., Metastatic immune-related genes for affecting prognosis and immune response in renal clear cell carcinoma, *Front. Mol. Biosci.*, **8** (2021), 794326. https://doi.org/10.3389/fmolb.2021.794326
37. J. Jing, J. Sun, Y. Wu, N. Zhang, C. Liu, S. Chen, et al., AQP9 is a prognostic factor for kidney cancer and a promising indicator for M2 TAM polarization and CD8+ T-cell recruitment, *Front. Oncol.*, **11** (2021), 770565. https://doi.org/10.3389/fonc.2021.770565
38. J. Song, Y. D. Liu, J. Su, D. Yuan, F. Sun, J. Zhu, Systematic analysis of alternative splicing signature unveils prognostic predictor for kidney renal clear cell carcinoma, *J. Cell Physiol.*, **234** (2019), 22753–22764. https://doi.org/10.1002/jcp.28840
39. G. Du, X. Yan, Z. Chen, R. J. Zhang, K. Tuoheti, X. J. Bai, et al., Identification of transforming growth factor beta induced (TGFBI) as an immune-related prognostic factor in clear cell renal cell carcinoma (ccRCC), *Aging (Albany NY)*, **12** (2020), 8484–8505. https://doi.org/10.18632/aging.103153
40. G. Chen, Y. Wang, L. Wang, W. Xu, Identifying prognostic biomarkers based on aberrant DNA methylation in kidney renal clear cell carcinoma, *Oncotarget*, **8** (2017), 5268–5280. https://doi.org/10.18632/oncotarget.14134
41. G. Lin, Q. Feng, F. Zhan, F. Yang, Y. Niu, G. Li, Generation and analysis of pyroptosis-based and immune-based signatures for kidney renal clear cell carcinoma patients, and cell experiment, *Front. Genet.*, **13** (2022), 809794. https://doi.org/10.3389/fgene.2022.809794
42. X. L. Xing, Y. Liu, J. Liu, H. Zhou, H. Zhang, Q. Zuo, et al., Comprehensive analysis of ferroptosis- and immune-related signatures to improve the prognosis and diagnosis of kidney renal clear cell carcinoma, *Front. Immunol.*, **13** (2022), 851312. https://doi.org/10.3389/fimmu.2022.851312
43. Y. Hong, M. Lin, D. Ou, Z. Huang, P. Shen, A novel ferroptosis-related 12-gene signature predicts clinical prognosis and reveals immune relevancy in clear cell renal cell carcinoma, *BMC Cancer*, **21** (2021), 831. https://doi.org/10.1186/s12885-021-08559-0
44. Y. Zhang, M. Tang, Q. Guo, H. Xu, Z. Yang, D. Li, The value of erlotinib related target molecules in kidney renal cell carcinoma via bioinformatics analysis, *Gene*, **816** (2022), 146173. https://doi.org/10.1016/j.gene.2021.146173
45. Y. L. Wang, H. Liu, L. L. Wan, K. H. Pan, J. X. Ni, Q. Hu, et al., Characterization and function of biomarkers in sunitinib-resistant renal carcinoma cells, *Gene*, **832** (2022), 146514. https://doi.org/10.1016/j.gene.2022.146514
46. X. Che, X. Qi, Y. Xu, Q. Wang, G. Wu, Using genomic and transcriptome analyses to identify the role of the oxidative stress pathway in renal clear cell carcinoma and its potential therapeutic significance, *Oxid. Med. Cell Longev.*, **2021** (2021), 5561124. https://doi.org/10.1155/2021/5561124
47. X. Che, X. Qi, Y. Xu, Q. Wang, G. Wu, Genomic and transcriptome analysis to identify the role of the mtor pathway in kidney renal clear cell carcinoma and its potential therapeutic significance, *Oxid. Med. Cell Longev.*, **2021** (2021), 6613151. https://doi.org/10.1155/2021/6613151

48. G. Tan, Z. Xuan, Z. Li, S. Huang, G. Chen, Y. Wu, et al., The critical role of BAP1 mutation in the prognosis and treatment selection of kidney renal clear cell carcinoma, *Transl. Androl. Urol.*, **9** (2020), 1725–1734. https://doi.org/10.21037/tau-20-1079
49. M. Huang, T. Zhang, Z. Y. Yao, C. Xing, Q. Wu, Y. W. Liu, et al., MicroRNA related prognosis biomarkers from high throughput sequencing data of kidney renal clear cell carcinoma, *BMC Med. Genomics*, **14** (2021), 72. https://doi.org/10.1186/s12920-021-00932-z
50. L. Peng, Z. Chen, Y. Chen, X. Wang, N. Tang, MIR155HG is a prognostic biomarker and associated with immune infiltration and immune checkpoint molecules expression in multiple cancers, *Cancer Med.*, **8** (2019), 7161–7173. https://doi.org/10.1002/cam4.2583
51. D. Zhang, S. Zeng, X. Hu, Identification of a three-long noncoding RNA prognostic model involved competitive endogenous RNA in kidney renal clear cell carcinoma, *Cancer Cell Int.*, **20** (2020), 319. https://doi.org/10.1186/s12935-020-01423-4
52. S. Khadirnaikar, P. Kumar, S. N. Pandi, R. Malik, S. M. Dhanasekaran, S. K. Shukla, Immune associated LncRNAs identify novel prognostic subtypes of renal clear cell carcinoma, *Mol. Carcinog.*, **58** (2019), 544–553. https://doi.org/10.1002/mc.22949
53. E. Clough, T. Barrett, The gene expression omnibus database, *Methods Mol. Biol.*, **1418** (2016), 93–110. https://doi.org/10.1007/978-1-4939-3578-9_5
54. M. E. Ritchie, B. Phipson, D. I. Wu, Y. Hu, C. W. Law, W. Shi, et al., Limma powers differential expression analyses for RNA-sequencing and microarray studies, *Nucleic Acids Res.*, **43** (2015), e47. https://doi.org/10.1093/nar/gkv007
55. Z. Jiang, M. Shao, X. Dai, Z. Pan, D. Liu, Identification of diagnostic biomarkers in systemic lupus erythematosus based on bioinformatics analysis and machine learning, *Front. Genet.*, **13** (2022), 865559. https://doi.org/10.3389/fgene.2022.865559
56. T. Wu, E. Hu, S. Xu, M. Chen, P. Guo, Z. Dai, et al., clusterProfiler 4.0: A universal enrichment tool for interpreting omics data, *Innovation*, **2** (2021), 100141. https://doi.org/10.1016/j.xinn.2021.100141
57. Gene Ontology Consortium, The Gene Ontology (GO) database and informatics resource, *Nucleic Acids Res.*, **32** (2004), D258–D261. https://doi.org/10.1093/nar/gkh036
58. D. Szklarczyk, A. L. Gable, D. Lyon, A. Junge, S. Wyder, J. Huerta-Cepas, et al., STRING v11: protein-protein association networks with increased coverage, supporting functional discovery in genome-wide experimental datasets, *Nucleic Acids Res.*, **47** (2019), D607–D613. https://doi.org/10.1093/nar/gky1131
59. P. Shannon, A. Markiel, O. Ozier, N. S. Baliga, J. T. Wang, D. Ramage, et al., Cytoscape: a software environment for integrated models of biomolecular interaction networks, *Genome Res.*, **13** (2003), 2498–2504. https://doi.org/10.1101/gr.1239303
60. W. Lin, Y. Tang, M. Zhang, B. Liang, M. Wang, L. Zha, et al., Integrated bioinformatic analysis reveals txnrd1 as a novel biomarker and potential therapeutic target in idiopathic pulmonary arterial hypertension, *Front. Med.*, **9** (2022), 894584. https://doi.org/10.3389/fmed.2022.894584
61. A. Subramanian, P. Tamayo, V. K. Mootha, S. Mukherjee, B. L. Ebert, M. A. Gillette, et al., Gene set enrichment analysis A knowledge-based approach for interpreting genome-wide expression profiles, *Proc. Natl. Acad. Sci.*, **102** (2005), 15545–15550. https://doi.org/10.1073/pnas.0506580102
62. Z. Zhuang, D. Li, M. Jiang, Y. Wang, Q. Cao, S. Li, et al., An integrative bioinformatics analysis of the potential mechanisms involved in propofol affecting hippocampal neuronal cells, *Comput. Intell. Neurosci.*, **2022** (2022), 4911773. https://doi.org/10.1155/2022/4911773
63. F. Ponten, K. Jirstrom, M. Uhlen, The Human Protein Atlas--a tool for pathology, *J. Pathol.*, **216** (2008), 387–393. https://doi.org/10.1002/path.2440

64. D. S. Chandrashekar, B. Bashel, S. A. H. Balasubramanya, C. J. Creighton, I. Ponce-Rodriguez, B. V. Chakravarthi, et al., UALCAN: a portal for facilitating tumor subgroup gene expression and survival analyses, *Neoplasia*, **19** (2017), 649–658. https://doi.org/10.1016/j.neo.2017.05.002
65. Z. Tang, C. Li, B. Kang, G. Gao, C. Li, Z. Zhang, GEPIA: a web server for cancer and normal gene expression profiling and interactive analyses, *Nucleic Acids Res.*, **45** (2017), W98–W102. https://doi.org/10.1093/nar/gkx247
66. Y. C. Yang, M. Y. Zhang, J. Y. Liu, Y. Y. Jiang, X. L. Ji, Y. Q. Qu, Identification of ferroptosis-related hub genes and their association with immune infiltration in chronic obstructive pulmonary disease by bioinformatics analysis, *Int. J. Chron. Obstruct. Pulmon. Dis.*, **17** (2022), 1219–1236. https://doi.org/10.2147/COPD.S348569
67. T. Li, J. Fu, Z. Zeng, D. Cohen, J. Li, Q. Chen, et al., TIMER2.0 for analysis of tumor-infiltrating immune cells, *Nucleic Acids Res*, **48** (2020), W509–W514. https://doi.org/10.1093/nar/gkaa407
68. B. A. Teicher, TGFbeta-directed therapeutics: 2020, *Pharmacol. Ther.*, **217** (2021), 107666. https://doi.org/10.1016/j.pharmthera.2020.107666
69. A. E. Vilgelm, A. Richmond, Chemokines modulate immune surveillance in tumorigenesis, metastasis, and response to immunotherapy, *Front. Immunol.*, **10** (2019), 333. https://doi.org/10.3389/fimmu.2019.00333
70. R. Wang, B. Zheng, H. Liu, X. Wan, Long non-coding RNA PCAT1 drives clear cell renal cell carcinoma by upregulating YAP via sponging miR-656 and miR-539, *Cell Cycle*, **19** (2020), 1122–1131. https://doi.org/10.1080/15384101.2020.1748949
71. S. Nagashima, J. Maruyama, K. Honda, Y. Kondoh, H. Osada, M. Nawa, et al., CSE1L promotes nuclear accumulation of transcriptional coactivator TAZ and enhances invasiveness of human cancer cells, *J. Biol. Chem.*, **297** (2021), 100803. https://doi.org/10.1016/j.jbc.2021.100803
72. P. Chen, Y. Duan, X. Lu, L. Chen, W. Zhang, H. Wang, et al., RB1CC1 functions as a tumor-suppressing gene in renal cell carcinoma via suppression of PYK2 activity and disruption of TAZ-mediated PDL1 transcription activation, *Cancer Immunol. Immunother.*, **70** (2021), 3261–3275. https://doi.org/10.1007/s00262-021-02913-8
73. S. Xu, H. Zhang, Y. Chong, B. Guan, P. Guo, YAP promotes VEGFA expression and tumor angiogenesis though Gli2 in human renal cell carcinoma, *Arch. Med. Res.*, **50** (2019), 225–233. https://doi.org/10.1016/j.arcmed.2019.08.010
74. P. Carter, U. Schnell, C. Chaney, B. Tong, X. Pan, J. Ye, et al., Deletion of Lats1/2 in adult kidney epithelia leads to renal cell carcinoma, *J. Clin. Invest.*, **131** (2021), e144108. https://doi.org/10.1172/JCI144108
75. S. Xu, H. Zhang, T. Liu, Z. Wang, W. Yang, T. Hou, et al., 6-Gingerol suppresses tumor cell metastasis by increasing YAP(ser127) phosphorylation in renal cell carcinoma, *J. Biochem. Mol. Toxicol.*, **35** (2021), e22609. https://doi.org/10.1002/jbt.22609
76. S. Xu, Z. Yang, Y. Fan, B. Guan, J. Jia, Y. Gao, et al., Curcumin enhances temsirolimus-induced apoptosis in human renal carcinoma cells through upregulation of YAP/p53, *Oncol. Lett.*, **12** (2016), 4999–5006. https://doi.org/10.3892/ol.2016.5376
77. M. D. Robinson, D. J. McCarthy, G. K. Smyth, edgeR: a Bioconductor package for differential expression analysis of digital gene expression data, *Bioinformatics*, **26** (2010), 139–140. https://doi.org/10.1093/bioinformatics/btp616
78. S. Anders, W. Huber, Differential expression analysis for sequence count data, *Genome Biol,*, **11** (2010), R106. https://doi.org/10.1186/gb-2010-11-10-r106
79. M. I. Love, W. Huber, S. Anders, Moderated estimation of fold change and dispersion for RNA-seq data with DESeq2, *Genome Biol.*, **15** (2014), 550. https://doi.org/10.1186/s13059-014-0550-8

80. D. W. Huang, B. T. Sherman, R. A. Lempicki, Systematic and integrative analysis of large gene lists using DAVID bioinformatics resources, *Nat. Protoc.*, **4** (2009), 44–57. https://doi.org/10.1038/nprot.2008.211
81. C. Xie, X. Mao, J. Huang, Y. Ding, J. Wu, S. Dong, et al., KOBAS 2.0: a web server for annotation and identification of enriched pathways and diseases, *Nucleic Acids Res.*, **39** (2011), W316–W322. https://doi.org/10.1093/nar/gkr483
82. Y. Zhou, B. Zhou, L. Pache, M. Chang, A. H. Khodabakhshi, O. Tanaseichuk, et al., Metascape provides a biologist-oriented resource for the analysis of systems-level datasets, *Nat. Commun.*, **10** (2019), 1523. https://doi.org/10.1038/s41467-019-09234-6
83. Y. Liao, J. Wang, E. J. Jaehnig, Z. Shi, B. Zhang, WebGestalt 2019: gene set analysis toolkit with revamped UIs and APIs, *Nucleic Acids Res.*, **47** (2019), W199–W205. https://doi.org/10.1093/nar/gkz401
84. M. D. Paraskevopoulou, G. Georgakilas, N. Kostoulas, M. Reczko, M. Maragkakis, T. M. Dalamagas, et al., DIANA-LncBase: experimentally verified and computationally predicted microRNA targets on long non-coding RNAs, *Nucleic Acids Res.*, **41** (2013), D239–D245. https://doi.org/10.1093/nar/gks1246
85. S. D. Hsu, F. M. Lin, W. Y. Wu, C. Liang, W. C. Huang, W. L. Chan, et al., miRTarBase: a database curates experimentally validated microRNA–target interactions, *Nucleic Acids Res.*, **39** (2011), D163–D169. https://doi.org/10.1093/nar/gkq1107
86. J. H. Yang, J. H. Li, P. Shao, H. Zhou, Y. Q. Chen, starBase: a database for exploring microRNA-mRNA interaction maps from Argonaute CLIP-Seq and Degradome-Seq data, *Nucleic Acids Res.*, **39** (2011), D202–D209. https://doi.org/10.1093/nar/gkq1056
87. W. Liu, Y. Jiang, L. Peng, X. Sun, W. Gan, Q. Zhao, et al., Inferring gene regulatory networks using the improved markov blanket discovery algorithm, *Interdiscip. Sci.*, **14** (2022), 168–181. https://doi.org/10.1007/s12539-021-00478-9
88. L. Zhang, P. Yang, H. Feng, Q. Zhao, H. Liu, Using Network Distance Analysis to Predict lncRNA-miRNA Interactions, *Interdiscip. Sci.*, **13** (2021), 535–545. https://doi.org/10.1007/s12539-021-00458-z
89. H. Liu, G. Ren, H. Chen, Q. Liu, Y. Yang, Q. Zhao, Predicting lncRNA–miRNA interactions based on logistic matrix factorization with neighborhood regularized, *Knowledge Based Syst.*, **191** (2020), 105261. https://doi.org/10.1016/j.knosys.2019.105261
90. W. Liu, H. Lin, L. Huang, L. Peng, T. Tang, Q. Zhao, et al., Identification of miRNA-disease associations via deep forest ensemble learning based on autoencoder, *Brief Bioinform.*, **23** (2022), bbac104. https://doi.org/10.1093/bib/bbac104
91. C. C. Wang, C. D. Han, Q. Zhao, X. Chen, Circular RNAs and complex diseases: from experimental results to computational models, *Brief Bioinform.*, **22** (2021), bbab286. https://doi.org/10.1093/bib/bbab286
92. A. Reustle, M. Di Marco, C. Meyerhoff, A. Nelde, J. S. Walz, S. Winter, et al., Integrative -omics and HLA-ligandomics analysis to identify novel drug targets for ccRCC immunotherapy, *Genome Med.*, **12** (2020), 32. https://doi.org/10.1186/s13073-020-00731-8
93. K. Dong, W. Chen, X. Pan, H. Wang, Y. Sun, C. Qian, et al., FCER1G positively relates to macrophage infiltration in clear cell renal cell carcinoma and contributes to unfavorable prognosis by regulating tumor immunity, *BMC Cancer*, **22** (2022), 140. https://doi.org/10.1186/s12885-022-09251-7

94. Y. Chen, F. He, R. Wang, M. Yao, Y. Li, D. Guo, et al., NCF1/2/4 are prognostic biomarkers related to the immune infiltration of kidney renal clear cell carcinoma, *Biomed. Res. Int.*, **2021** (2021), 5954036. https://doi.org/10.1155/2021/5954036
95. B. G. Kim, E. Malek, S. H. Choi, J. J. Ignatz-Hoover, J. J. Driscoll, Novel therapies emerging in oncology to target the TGF-beta pathway, *J. Hematol. Oncol.*, **14** (2021), 55. https://doi.org/10.1186/s13045-021-01053-x
96. J. D. Richter, X. Zhao, The molecular biology of FMRP: new insights into fragile X syndrome, *Nat. Rev. Neurosci.*, **22** (2021), 209–222. https://doi.org/10.1038/s41583-021-00432-0
97. Y. Laitman, L. Ries-Levavi, M. Berkensdadt, J. Korach, T. Perri, E. Pras, et al., FMR1 CGG allele length in Israeli BRCA1/BRCA2 mutation carriers and the general population display distinct distribution patterns, *Genet. Res.*, **96** (2014), e11. https://doi.org/10.1017/S0016672314000147
98. W. Li, L. Zhang, B. Guo, J. Deng, S. Wu, F. Li, et al., Exosomal FMR1-AS1 facilitates maintaining cancer stem-like cell dynamic equilibrium via TLR7/NFkappaB/c-Myc signaling in female esophageal carcinoma, *Mol. Cancer*, **18** (2019), 22. https://doi.org/10.1186/s12943-019-0949-7
99. Y. Jiang, Z. Wang, C. Ying, J. Hu, T. Zeng, L. Gao, FMR1/circCHAF1A/miR-211-5p/HOXC8 feedback loop regulates proliferation and tumorigenesis via MDM2-dependent p53 signaling in GSCs, *Oncogene*, **40** (2021), 4094–4110. https://doi.org/10.1038/s41388-021-01833-2
100. Z. Shen, B. Liu, B. Wu, H. Zhou, X. Wang, J. Cao, et al., FMRP regulates STAT3 mRNA localization to cellular protrusions and local translation to promote hepatocellular carcinoma metastasis, *Commun. Biol.*, **4** (2021), 540. https://doi.org/10.1038/s42003-021-02071-8
101. Y. Higuchi, M. Ando, A. Yoshimura, S. Hakotani, Y. Koba, Y. Sakiyama, et al., Prevalence of fragile X-associated tremor/ataxia syndrome in patients with cerebellar ataxia in Japan, *Cerebellum*, (2021), 1–10. https://doi.org/10.1007/s12311-021-01323-x
102. K. H. Yu, N. Palmer, K. Fox, L. Prock, K. D. Mandl, I. S. Kohane, et al., The phenotypical implications of immune dysregulation in fragile X syndrome, *Eur. J. Neurol.*, **27** (2020), 590–593. https://doi.org/10.1111/ene.14146
103. M. Careaga, D. Rose, F. Tassone, R. F. Berman, R. Hagerman, P. Ashwood, Immune dysregulation as a cause of autoinflammation in fragile X premutation carriers: link between FMRI CGG repeat number and decreased cytokine responses, *PLoS One*, **9** (2014), e94475. https://doi.org/10.1371/journal.pone.0094475
104. S. L. Hodges, S. O. Nolan, L. A. Tomac, I. D. Muhammad, M. S. Binder, J. H. Taube, et al., Lipopolysaccharide-induced inflammation leads to acute elevations in pro-inflammatory cytokine expression in a mouse model of Fragile X syndrome, *Physiol. Behav.*, **215** (2020), 112776. https://doi.org/10.1016/j.physbeh.2019.112776
105. S. L. Hodges, S. O. Nolan, J. H. Taube, J. N. Lugo, Adult Fmr1 knockout mice present with deficiencies in hippocampal interleukin-6 and tumor necrosis factor-alpha expression, *Neuroreport*, **28** (2017), 1246–1249. https://doi.org/10.1097/WNR.0000000000000905

AIMS Press